Thin-Walled Structures 94 (2015) 293–301

Contents lists available at ScienceDirect

Thin-Walled Structures

journal homepage: www.elsevier.com/locate/tws

On the methods of critical load estimation of spherical circle axially symmetrical shells

J. Awrejcewicz [a,b,*], A.V. Krysko [c], I.V. Papkova [d], I.Y. Vygodchikova [d], V.A. Krysko [d]

[a] Department of Automation, Biomechanics and Mechatronics, Lodz University of Technology, 1/15 Stefanowski St., 90-924 Lodz, Poland
[b] Warsaw University of Technology, Department of Vehicles, 84 Narbutt Str., 02-524 Warsaw, Poland
[c] Department of Applied Mathematics and Systems Analysis, Saratov State Technical University, Politekhnicheskaya 77, 410054 Saratov, Russian Federation
[d] Department of Mathematics and Modeling, Saratov State Technical University, Politekhnicheskaya 77, 410054 Saratov, Russian Federation

ARTICLE INFO

Article history:
Received 17 June 2014
Received in revised form
30 March 2015
Accepted 2 April 2015

Keywords:
Stability
Shells
Critical loads
Chebyshev's method

ABSTRACT

A relaxation method is applied to estimate and predict a critical set of parameters responsible for stability loss (buckling) of spherical circle axially symmetric shells. The buckling phenomenon under static loading was investigated by solving the Cauchy problem for a set of ordinary differential equations and the Hausdorff metrics was applied while quantifying the data obtained within the novel approach.

1. Introduction

One of the key issues in the field of materials strength and structural mechanics is that devoted to the study of stability as well as buckling and postbuckling behavior of structural members such as beams, plates, shells and thin-walled structures. These members of structures and the structures themselves are usually subjected either to static or dynamic, or both types of loading, and hence various computational techniques, including numerical, analytical and combined numerical–analytical approaches are used to analyze various types of stability loss including local, global (flexural, torsional, lateral, distorsional and their combinations) and interactive forms of buckling.

It is well known that the mentioned either isolated or coupled structural members have found wide applications in numerous constructions in aerospace, civil engineering, ship building, automobiles, aircraft wings and fuselages, and others. There are numerous papers/monographs devoted to stability loss (and buckling) investigation of structural members treated as isolated or interacting objects, where the structural members are linked with each other by different/mixed boundary conditions. It is well recognized that stability loss is understood as the transition of a mechanical system from one to another equilibrium configuration either in a smooth way (bifurcation point) or by a sudden jump from a stable to unstable equilibrium path (limit point).

In general, there are either static or dynamic loads. The latter ones are measured via "pulse intensity" and "pulse velocity". Depending on their length in time, different dynamic loading phenomena can be distinguished. Namely, when pulse duration is short (long) and the amplitude is relatively high (average) then an impact (quasi-static) behavior is observed. In the case when the pulse duration is close to the period of natural vibrations, a dynamic buckling takes place.

It should be emphasized that a finite duration load may have different shapes (parabolic, triangular, rectangular, exponential or even irregular), since it attempts to model real dynamic load met in nature and engineering applications. Studies on the stability and buckling behavior of mainly thin-walled structures date back to over a hundred years, and were motivated by Bernoulli/Euler [1], Timoshenko [2] and Volmir [3,4]. Here, our studies are limited to only a few proposals regarding stability phenomena, but the reader may find more information for instance in the recent monograph of Kubiak [5].

Growing interest in stability loss/buckling/postbuckling behavior of thin-walled structures measured by the publication of a number of papers/books began in the 1970s (see for instance [6–12]). In particular, a lot of research was aimed at non-linear problems of stability of orthotropic and anisotropic thin-walled structures. The studies covered orthotropic plate buckling [13], critical stresses of anisotropic laminated plates [14], buckling of composite and anisotropic plates [15–17], stability of columns and square laminate plates [18] and postbuckling behavior of

* Corresponding author.
E-mail addresses: awrejcew@p.lodz.pl (J. Awrejcewicz), anton.krysko@gmail.com (A.V. Krysko), ikravzova@mail.ru (I.V. Papkova), VigodchikovaIY@info.sgu.ru (I.Y. Vygodchikova), tak@san.ru (V.A. Krysko).

http://dx.doi.org/10.1016/j.tws.2015.04.003
0263-8231/

orthotropic laminated plates [19]. Numerous papers have been devoted to the solution of stability problem using numerical and analytical–numerical methods often applying commercial programs based on the finite elements method (FEM). However, despite the mentioned research aiming at the explanation of the static/dynamic stability loss of thin-walled structures and structural members, there is no a general stability definition/criterion formulated which can be validated experimentally and can satisfy engineering requirements regarding the load carrying capacity as well as stability of the mentioned mechanical objects. Below, a few of stability loss criteria regarding continuous mechanical objects which found considerable resonance among researchers are briefly illustrated and discussed.

Volmir [4] proposed a time-consuming though simple approach to determine the critical load while investigating dynamics of a simply supported rectangular plate subjected to pulses of infinite/finite durations and of rectangular/exponential shapes. He pointed out that the plate subjected to pulse load lost its stability, when the maximum deflection of the plate was equal to the assumed constant value (usually, it was either the plate thickness or the half-plate thickness). Budiansky and Hutchinson [20,21] and Budiansky and Roth [22] proposed displacement criteria regarding cylindrical shells axially loaded rods and cylindrical shells loaded transversally, respectively. There are two equivalent formulations of their criteria: 1) structures subjected to pulse loading lose their stability when an unlimited increase of their deflection for small load increments is observed; 2) a plate exhibits dynamic stability loss when its maximum deflection grows rapidly under a small load amplitude variation.

Both theoretical and experimental investigations of thin plates clamped on all contours and subjected to pulse load with a half-wave of sine shape carried out by Ari-Gur and Simonetta [23] yielded other four dynamic criteria. Only two of them are recalled (the other two deal with failures): 1) dynamic buckling takes place when a small increase of the loading pulse intensity causes a significant increase of the deflection value; 2) dynamic buckling takes place when a small increase of the pulse loading amplitude causes a decrease of the deflection value.

The so far discussed stability loss criteria concern isolated structural members like beams, columns, plates and shells. In complex structures composed of the linked simple structural members the problem is more difficult. One buckling mode may simply create other modes, and then a problem of multi-modal modes stability appears. Petry and Fahlbusch [24] extended the Budiansky–Hutchinson criterion to plated structures, and they proposed the following dynamic buckling criterion: *Dynamic response of a structure subjected to pulse load is dynamically stable if the condition that the equivalent stress* (originally the authors used the Huber–Mises hypothesis) *less/equal to the assumed limit of stress is satisfied at any time and any point of the structure.*

In addition to the presented status of existing criteria of the structural members stability loss, a few papers from the Russian literature are referred to. Kulikov [25] studied the stability of a spherical shell putting emphasis on numerical techniques applied to study non-linear behavior of thin elastic shells. Numerous algorithms of the FDM (Finite Difference Method) devoted to the solution of stability problems of mechanical structures allow researchers to solve a large class of static and dynamic problems. Valishvili [26] solved the static problem, where the non-linear boundary value problem was reduced to that of solving non-linear algebraic equations. In addition, static problems of structural membranes can be solved with the help of a relaxation method first applied by Feodos'ev for shells [27].

The so far given review of papers devoted to stability/buckling problems of structural members shows that there are numerous approaches to define and predict this phenomenon. However, it is also clear that none of them is sufficient and meets expectations of the engineering community. In general, models of the processes associated with stability loss of mechanical structures require derivation of complex variational equations or equivalent differential equations. Additionally, in spite of a large number of algorithms devoted to the computation of various kinds of stability loss and in spite of the used characteristics such as graphical stability loss visualization versus the applied load, there is no relatively simple and reliable estimation of stability loss pictures being validated by various laboratory experiments.

The aim of this paper is to get reliable characteristics of time evolution of the development of shell deformation versus the applied load variation in order to detect the critical load values. For this purpose the following problems are solved: (i) to estimate the deformation velocity while changing an input load; (ii) to get information on rapid changes of the deformation velocity development in order to reach a certain critical load level; (iii) to get information on the absolute and relative error introduced by the linear approximating function while changing the initial input. It should be emphasized the static problems are solved by using the dynamic method which is much more efficient in comparison to the standard static approaches.

The paper is organized in the following manner. In Section 2 both the method and algorithm of computation of an axially symmetric spherical shell are presented. Section 3 deals with a static stability loss of shells. A core of the paper is in Section 4 devoted to the application of modified Chebyshev's method used to quantify the velocity characteristics of shell deflection. In particular, an important theorem is formulated. Section 5 presents computational experiments validating the previous theoretical considerations. Concluding remarks sum up the research carried out and the novel results obtained.

2. Method and algorithm of computation

Consider a shallow spherical axially symmetrical shell described by the 2D space in R^2 in the polar co-ordinates introduced in the following way: $\Omega=\{(r,z)|\, r\in[0,b],\ -H/2\le z\le H/2\}$.

Dynamics of the mentioned axially symmetric shells is governed by the following set of PDEs:

$$\begin{aligned} w''+\varepsilon w' &= -\frac{\partial^4 w}{\partial r^4}-\frac{2}{r}\frac{\partial^3 w}{\partial r^3}+\frac{1}{r^2}\frac{\partial^2 w}{\partial r^2}-\frac{1}{r^3}\frac{\partial w}{\partial r}-\frac{\Phi}{r}\left(1-\frac{\partial^2 w}{\partial r^2}\right)\\ &\quad -\frac{\partial \Phi}{\partial r}\left(1-\frac{1}{r}\frac{\partial w}{\partial r}\right)-4q,\frac{\partial^2 \Phi}{\partial r^2}+\frac{1}{r}\frac{\partial \Phi}{\partial r}-\frac{1}{r^2}\frac{\partial \Phi}{\partial r}\\ &= \frac{\partial w}{\partial r}\left(1-\frac{1}{2r}\frac{\partial w}{\partial r}\right), \end{aligned} \tag{2.1}$$

where $\Phi=\partial F/\partial r$ and F stands for the stress (Airy's) function. While investigating theoretically real shells, usually a 3D problem of the theory of elasticity is reduced to that of 2D assuming that the shell material is elastic and satisfies Hook's law and that the Kirchhoff–Love hypothesis is validated (normals to the middle shell surface are not deformed with shell deformation).

System (2.1) is recast into its counterpart dimensionless form by introducing the following relations:

$$\bar{t}=\omega_0 t,\ \ \omega_0=\sqrt{\frac{Eg}{\gamma R^2}},\ \ \bar{\varepsilon}=\sqrt{\frac{g}{\gamma}}\frac{R}{EH}\varepsilon,\ \ \overline{F}=\eta_{\frac{F}{EH^3}},\ \ \overline{w}=\sqrt{\eta}_{\frac{w}{H}},\ \ \bar{r}=b_{\frac{r}{c}},$$
$$\bar{q}=\tfrac{\sqrt{\eta}}{4}\tfrac{q}{E}\left(\tfrac{R}{H}\right)^2,\ \ \eta=12(1-\nu^2),\ \ b=\sqrt[4]{\eta}_{\frac{c}{\sqrt{RH}}},$$

where t – time, ε – damping coefficient, F – stress function, w – displacement function, R – main shell curvature radius, $2c$ – length of ends of the shell curvature (see Fig. 1), $H=2h$ – shell thickness (see Fig. 1), b – shallow parameter, ν – Poisson's coefficient, r– distance between the axis of rotation and a point of the middle

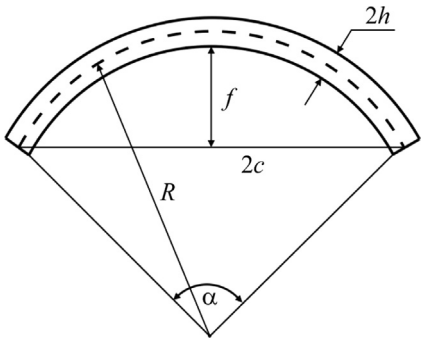

Fig. 1. The computational model of a shallow spherical axially symmetric shell.

shell surface, q – uniformly distributed load applied to the shell surface. For simplicity, bars in Eq. (2.1) over the dimensionless quantities have been already omitted, differentiation with respect to time is denoted by $d/dt = '$. Boundary and initial conditions should be added at the shell top. For simple–movable support in the meridian direction the boundary conditions have the following form:

$$\Phi = w = 0, \quad \frac{\partial^2 w}{\partial r^2} + \frac{\nu}{r} w = 0, \quad \text{for } r = b, \tag{2.2}$$

whereas initial conditions are as follows:

$$w = f_1(r,0), \quad w' = f_2(r,0), \quad 0 \le t < \infty. \tag{2.3}$$

In the small neighborhood of the shell center the following estimation holds:

$$\Phi \approx Ar, \quad \Phi' \approx A, \quad w \approx B + Cr^2, \quad w' \approx 2Cr, \quad w'' \approx 2C, \quad w''' \approx 0. \tag{2.4}$$

In order to reduce continuous system (2.1)–(2.4) to the system with lumped parameters the finite difference method (FDM) with approximation $O(\Delta^2)$ is applied. System (2.1)–(2.4) is recast into its counterpart finite-difference form with respect to r, i.e.,

$$\begin{aligned} w_i'' + \varepsilon w_i' = & -\frac{w_{i+1} - w_{i-1}}{2\Delta}\left(\frac{1}{r_i^3} - \frac{\Phi_{i+1} - \Phi_{i-1}}{2r_i\Delta}\right) \\ & + \frac{w_{i+1} - 2w_i + w_{i-1}}{r_i \Delta^2}\left(\Phi_i + \frac{1}{r_i}\right) - \frac{\Phi_{i+1} - \Phi_{i-1}}{2\Delta} - \frac{\Phi_i}{r_i} \\ & - \frac{w_{i+2} - 4w_{i+1} + 6w_i - 4w_{i-1} + w_{i-2}}{\Delta^4} \\ & - \frac{w_{i+2} - 2w_{i+1} + 2w_{i-1} - w_{i-2}}{r_i \Delta^3} - 4q_i, \\ \Phi_{i+1}\left(-\frac{1}{\Delta^2} - \frac{1}{2r_i\Delta}\right) + \Phi_i\left(\frac{2}{\Delta^2} + \frac{1}{r_i^2}\right) + \Phi_{i-1}\left(-\frac{1}{\Delta^2} + \frac{1}{2r_i\Delta}\right) & \\ = -\frac{w_{i+1} - w_{i-1}}{2\Delta}\left(1 - \frac{w_{i+1} - w_{i-1}}{4r_i\Delta}\right), & \end{aligned} \tag{2.5}$$

where $\Delta = b/n$ and n denotes a number of shell radius partitions. The boundary conditions take the form

$$\Phi_n = 0, \quad w_{n+1} = -w_{n-1}, \quad w_n = 0 \quad \text{for } r_n = b, \tag{2.6}$$

whereas the initial conditions are as follows:

$$w_n = f_1(r_k,0), \quad w_n' = f_2(r_k,0), \quad 0 \le k \le n, \quad 0 \le t < \infty. \tag{2.7}$$

Neglecting small terms and substituting differential operators by the central finite-difference for $r = \Delta$,the following conditions hold at the shell center:

$$\Phi_0 = \Phi_2 - 2\Phi_1, \quad w_0 = \frac{4}{3}w_1 - \frac{1}{3}w_2, \quad w_{-1} = \frac{8}{3}w_1 - \frac{8}{3}w_2 + w_3. \tag{2.8}$$

Though the applied load can be taken arbitrarily with respect to both spatial co-ordinate and time, only the static case is considered here, i.e. $q = const$. In order to solve the Cauchy problem (2.5)–(2.8) it is sufficient to apply the fourth-order Runge–Kutta method. In order to keep solution stability, the integration time step ($\Delta t = 3.90625 \cdot 10^{-3}$) was taken. In the numerical experiment $\Delta = 0.2$ with respect to the spatial co-ordinate was also taken. Though a discussion of reliability and validation of the obtained results, as well as a motivation of the choice of time and spatial steps are omitted here, one may follow the same algorithm of analysis in the papers [28–30].

3. Stability of shells (static case)

The following assumptions are taken into account while carrying out the computations of the shell/plate structural member.

1. Shell/plate should be thin. Owing to the definition introduced by Novozhilov [31], a shell is called thin, where maximum values of the ratio h/R (where R denotes the main shell curvature radius) are essentially less than one (1). He suggests also that it is reasonable to introduce the relative error of 5% for technical computations, which implies that the shells are treated as thin-walled structural members if the following inequality holds $h/R \le 1/40$. Otherwise, a shell will be understood as thick. The majority of shells applied in engineering satisfy the following estimation $1/2000 \le h/R \le 1/100$, and hence they can be treated as thin-walled.
2. In the case of shallow spherical shells our computational results refer to the geometrical data for shallow spherical axially symmetrical shell reported in Fig. 1. The studied shells can be considered as thin-walled shells if either the Reissner [32] hypothesis $f/2c \le 1/8$ or the Vlasov [33] hypothesis $f/2c \le 1/5$ holds. Now, if the Reissner assumption regarding shallow-shape criterion ($< \alpha = 60^\circ$) is taken, the following inequality $2c \le R$ is obtained (this can be directly derived from Fig. 1).

In order to solve static problems of the theory of plates and shells, traditionally a variety of approximating methods are applied. The latter ones allow us to reduce PDEs to ANE, i.e. partial differential equations to algebraic non-linear equations, where the equations obtained are further linearized.

Owing to the relaxation method, a solution to a system of PDEs is reduced to the equivalent Cauchy problems of ODE's [34]. The main idea of the relaxation method originally proposed by Feodos'ev [27,34] is as follows: for $\varepsilon = \varepsilon_{cr} = 0.9$ relation $\{q_m,\ w_m(t)\}$ is constructed, where $m = 1, 2, \ldots$ denotes the static load values number for which a solution was obtained using the relaxation method, i.e. using the dynamic approach and taking into account a relatively high damping coefficient ε. An increase in the number of iterations, i.e. the number of m, implies more smoothened curve $\{q_m,\ w_m(t)\}$, and hence a critical load value associated with buckling is more accurately estimated. This allows us to construct characteristics $q(w_{st})$, and to study further the stress–strain state of the construction being analyzed. In other words, the method of dynamics is applied here to solve the problems of statics. Observe that for high damping term ε_{cr}, the shell dynamics is quickly damped, and the static equilibrium position is found in a simple and relatively fast way by applying the relaxation method. In the four given examples it is easy to follow how $w_m(t)$ tends to the corresponding w_{st}.

In Ref. [35] advantages of the employed method over the widely used Newton's method and other iterational approaches are outlined. The applied relaxation method is used to detect non-symmetric solutions for shells rectangular in plane. In order to demonstrate computational benefits of the relaxation method applied here, four numerical examples have been studied.

Example 1. A steel flexible shell circular in plane with a simple–movable support having the following geometric and physical parameters: $c=0.055\ m$, $\nu=0.3$, $h=0.003\ m$, $E=210\ GPa$, $b\approx 4$, $R=0.2\ m$ is considered.

Fig. 2 shows deflection $w(t)$ obtained for the case of the static load action (left) and the dependence $q(w_{st})$ (right) for the dimensional quantities and parameters. Three curves $w(t)$ for the constant loads $q=57;\ 59.5;\ 60.6$ show that the solutions tend to the three constant values of shell deflection w_m yielded by both static (w_{st}) and dynamic (w_m) approaches applied. In particular, it is shown how a small change of q implies a sudden snap-through transition to another equilibrium of shell configurations (compare the time histories in red and blue).

Fig. 3 shows relations $q(w)$ obtained using the relaxation algorithm (a,c) and the method proposed by Valishvili [26] (b) for boundary conditions given in this figure, and for the fixed value of parameter $b=4$, which validates the obtained results by solving PDEs in time.

However, the dynamic relaxation approach applied here makes it possible to estimate critical loads with high accuracy, and to define directly if the buckling appears inside or outside the shell surface. Loops of the characteristics $q_0(w)$ may occur (see Example 3) because they are constructed regarding the shell center, whereas the remaining points of the shell radius may behave individually, i.e. the shell stability loss may occur not in the shell center but in the shell quadrants. In the latter case the loops describe the behavior of the shell center as a result of stability loss in the shell quadrants.

The curves $q(w)$ obtained by our relaxation method (a,c) and these attained using the Valishvili approach [26] concern a simple movable shell support (Fig. 3) for $b=4$ and they almost fully coincide. Observe that the reported solution obtained by the Valishvili method is non-unique not only with respect to the load but also with respect to deflection, and it cannot yield proper values of either upper or bottom critical load estimation.

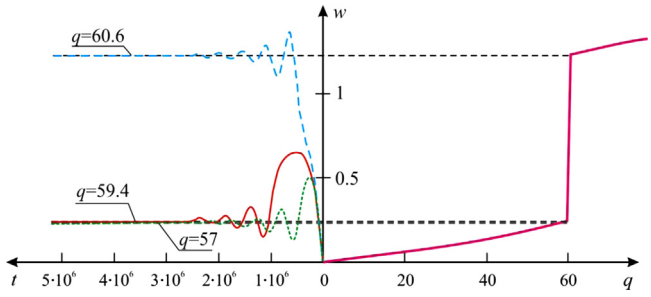

Fig. 2. Shell center deflection versus load obtained via dynamic (left) and static (right) approaches (Example 1). (For interpretation of the references to color in this figure the reader is referred to the web version of this article.)

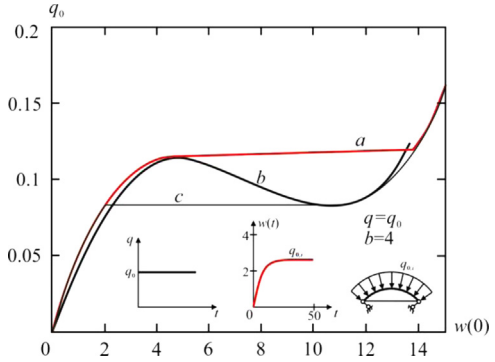

Fig. 3. A shell with simple and movable support $(q=q_0)$.

Example 2. A steel flexible shell circular in plane with a simple–movable support and with the following geometric and physical parameters: $c=0.13\ m$, $\nu=0.3$, $h=0.003\ m$, $E=210\ GPa$, $b\approx 8$, $R=0.3$ m, is considered. $w_m(t)$ and $w_{st}(q)$ for $q=25.45;\ 35;\ 35.5$ were computed in a way similar to that described in Example 1.

In this case (Fig. 4) the numerical results obtained via static and dynamic approaches coincide very well and a sudden jump (snap through) is demonstrated (compare blue and red time histories). Deflection forms $w(r)$ of the shell for the critical load ($q=35$) and for the static stability loss are reported in Fig. 5. In the case of the critical load the shell exhibits deflections in the quadrants (blue), whereas after stability loss the maximum shell deflection is achieved in the shell center (red).

Example 3. A steel flexible shell circular in plane with a simple–movable support and with the following geometric and physical parameters: $c=0.25\ m$, $\nu=0.3$, $h=0.004\ m$, $E=210\ GPa$, $b\approx 10$, $R=0.5$ m, is studied. A comparison of results obtained by Newton's method [26] and the applied relaxation method (red) is reported in Fig. 6 (non-dimensional quantities). In addition, Fig. 7 gives the shell deflection forms in the case of the critical load (blue) and after static stability loss (red).

Example 4. A steel flexible shell circular in plane with the simple/movable and movable support and with the following fixed parameters: $c=0.2\ m$, $\nu=0.3$, $h=0.0018\ m$, $E=210\ GPa$, $b\approx 12$, $R=0.5\ m$, $h/R=0.004$ (thin shell), and $2c=40<R$ (shallow shell) is analyzed. Fig. 8 illustrates $\overline{q}(\overline{w})$ (non-dimensional) dependencies obtained via Newton's method versus the employed relaxation method (green and red). On the other hand, Fig. 9 shows shell deflection form subjected to critical load (blue) and after the static stability loss (red).

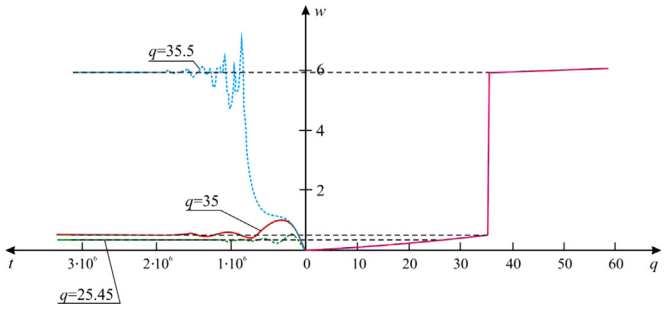

Fig. 4. Shell center deflection versus load obtained via dynamic (left) and static (right) approaches (Example 2). (For interpretation of the references to color in this figure the reader is referred to the web version of this article.)

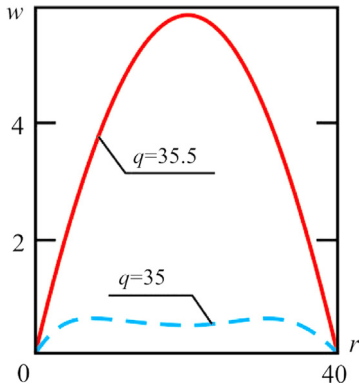

Fig. 5. Shell deflection form $w(r)$ for Example 2. (For interpretation of the references to color in this figure the reader is referred to the web version of this article.)

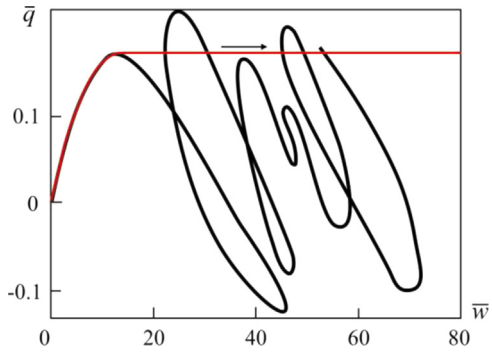

Fig. 6. Dependencies $\bar{q}(\overline{w})$ obtained via dynamic and static approaches. (For interpretation of the references to color in this figure legend, the reader is referred to the web version of this article.)

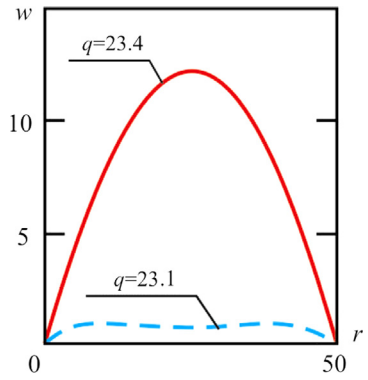

Fig. 7. Shell deflection form $w(r)$ for Example 3.(For interpretation of the references to color in this figure the reader is referred to the web version of this article.)

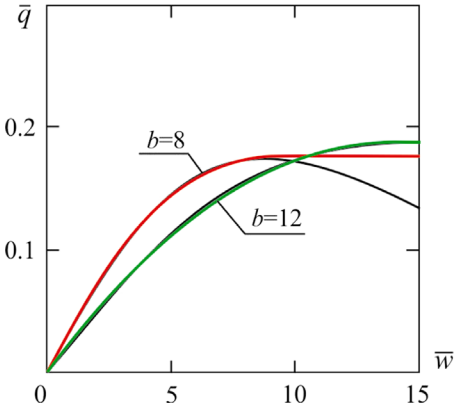

Fig. 8. Dependencies $\bar{q}(\overline{w})$ for different b obtained using dynamic (red and green) and static approaches. (For interpretation of the references to color in this figure legend, the reader is referred to the web version of this article.)

In this work a novel approach to the computation of a critical load, where shell stability loss takes place, is proposed. This method yields results at least few times faster than the known traditional methods. Besides, this method relies only on the initial short time interval monitoring (where the vibrational process is yet unstationary), while estimating the occurrence of buckling.

Table 1 gives numerical results. The static load values are: $q=0.025$, 0.05, 0.075, 0.1, 0.125 and 0.15. The buckling phenomenon takes place when the load is changed from $q=0.125$ (pre-critical load) to $q=0.15$ (post-critical load).

In Table 1, on the basis of Fig. 3, different values of the applied load with a simultaneous relative error estimation are reported. The proposed and applied novel method for computation of the critical load allows us not only to reduce the computational time,

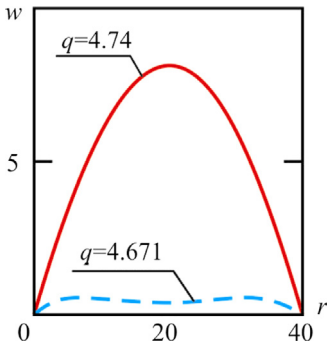

Fig. 9. Shell deflection form $w(r)$ for Example 4. (For interpretation of the references to color in this figure the reader is referred to the web version of this article.)

but also to carry out an analysis based on the shell deformation for only a few values of the applied load.

The obtained experimental data shown in Table 1 are further analyzed from the point of view of their compression. This allows us to obtain novel quantifying characteristics principally different from the known static quantification tools, and provides important information on the rate of linear deformation development together with the estimation of maximum absolute approximation error. As it will be shown further, these characteristics make it finally possible to estimate the critical loads.

4. Modified Chebyshev's method and shell velocity characteristics

The problem regarding the best and uniform approximation of a function via algebraic polynomials was formulated by Chebyshev already in 1854. Here, its discrete variant is revisited briefly (see [36], page 13).

Let a series of function values $y_k=y(t_k)$, $k\in 0,\ldots,N$ on the interval $T=\{t_0<t_1<\ldots<t_N\}$ be given, and let natural number n of the algebraic polynomial $p_n(A,t)$ be fixed. The aim is to find minimum deviations between all grid node values of the discrete functions and the approximating polynomial values.

$$\rho=\min_{A\in R^{n+1}}\max_{k\in 0,\ldots,N}|y_k-p_n(A,t_k)|. \tag{4.1}$$

Problem (4.1) has been solved for different polynomial orders, and then generalized through the introduction of additional constraints to the approximating polynomial (see Ref. [37] for more details). Below, a linear variant of problem (4.1) is considered and a few additional properties of the approximating function of linear-type problem (4.1) with constraints are applied.

The aim is to best approximate data (x_i,y_i), $i=1,\ldots,n$ by linear equation $\hat{y}=a_0+a_1x$. Points (x_i,y_i) do not lie exactly on the line, contrary to points $(x_i,\hat{y}_i)$, where $\hat{y}_i=a_0+a_1x_i$. Error in the i-th point is described by a difference between real and computational values $\varepsilon_i=y_i-\hat{y}_i$. A linear regression model has the form of $y_i=\beta_0+\beta_1x_i+\varepsilon_i$.

Since random errors ε_i cannot be measured, coefficients a_0, a_1 based on the existing data (x_i,y_i), $i=1,\ldots,n$ should be estimated. Mainly, the so called least squares method is applied. In order to estimate unknown parameters a_0, a_1, the following conditions should be satisfied:

$$Q(a_0,a_1)=\sum_{i=1}^{n}(y_i-\hat{y}_i)^2=\sum_{i=1}^{n}(y_i-a_0-a_1x_i)^2\to\min_{a_0,a_1}. \tag{4.2}$$

Sometimes (in economy) in order to achieve reliable events, both orthogonal polynomials and dynamic models are applied.

Table 1
Numerical results (first excitation).

$q=0.025$	$w(0.5,t)$	$q=0.05$	$w(0.5,t)$	$q=0.075$	$w(0.5,t)$	$q=0.1$	$w(0.5,t)$	$q=0.125$	$w(0.5,t)$	$q=0.15$	$w(0.5,t)$
t		t		t		t		t		t	
0	0	0	0	0	0	0	0	0	0	0	0
0.5	0.010823	0.5	0.000469	0.5	0.001054	0.5	0.001874	0.5	0.002929	0.5	0.004217
1	0.032029	1	0.004104	1	0.009235	1	0.016419	1	0.025657	1	0.036949
1.5	0.071351	1.5	0.020361	1.5	0.045808	1.5	0.08143	1.5	0.127225	1.5	0.183191
2	0.12643	2	0.06396	2	0.143963	2	0.256028	2	0.400194	2	0.5765
2.5	0.179835	2.5	0.129741	2.5	0.292764	2.5	0.521967	2.5	0.817901	2.5	1.181113
3	0.229558	3	0.212388	3	0.481468	3	0.862317	3	1.357318	3	1.968802
3.5	0.269709	3.5	0.295218	3.5	0.673864	3.5	1.215198	3.5	1.925795	3.5	2.812329
4	0.300431	4	0.369093	4	0.848954	4	1.542788	4	2.463958	4	3.62632
4.5	0.328474	4.5	0.444445	4.5	1.029921	4.5	1.88587	4.5	3.035261	4.5	4.50229
5	0.352623	5	0.516159	5	1.205604	5	2.225557	5	3.611824	5	5.403161
5.5	0.373114	5.5	0.582592	5.5	1.372155	5.5	2.554819	5.5	4.182884	5.5	6.314365
6	0.390387	6	0.643698	6	1.530466	6	2.877264	6	4.757677	6	7.255104
6.5	0.402867	6.5	0.692434	6.5	1.663584	6.5	3.161426	6.5	5.286137	6.5	8.153994
7	0.412074	7	0.731565	7	1.775929	7	3.412222	7	5.771766	7	9.011584
7.5	0.419226	7.5	0.764327	7.5	1.874462	7.5	3.641265	7.5	6.232213	7.5	9.853258
8	0.424676	8	0.791112	8	1.958908	8	3.846149	8	6.660529	8	10.66584
8.5	0.429205	8.5	0.814559	8.5	2.035387	8.5	4.037568	8.5	7.073153	8.5	11.47258
9	0.432667	9	0.83429	9	2.10366	9	4.216452	9	7.473662	9	12.28299
9.5	0.435074	9.5	0.849863	9.5	2.161841	9.5	4.377887	9.5	7.853053	9.5	13.08356
10	0.436743	10	0.862265	10	2.211883	10	4.524895	10	8.214988	10	13.87972
10.5	0.437791	10.5	0.871773	10.5	2.254112	10.5	4.657352	10.5	8.558726	10.5	14.6712
11	0.43854	11	0.879381	11	2.290168	11	4.776629	11	8.883678	11	15.45433
11.5	0.439115	11.5	0.885769	11.5	2.321997	11.5	4.886487	11.5	9.19545	11.5	16.23703
12	0.439495	12	0.890947	12	2.349782	12	4.987495	12	9.495334	12	17.02247
12.5	0.439752	12.5	0.895198	12.5	2.374157	12.5	5.080516	12.5	9.783884	12.5	17.81135
13	0.439871	13	0.898537	13	2.395344	13	5.166256	13	10.06266	13	18.60792
13.5	0.439887	13.5	0.901047	13.5	2.413424	13.5	5.244512	13.5	10.33115	13.5	19.41257
14	0.439881	14	0.903051	14	2.429016	14	5.316114	14	10.58943	14	20.22553
14.5	0.439855	14.5	0.904644	14.5	2.442531	14.5	5.38175	14.5	10.83865	14.5	21.04929
15	0.439826	15	0.905933	15	2.454298	15	5.441956	15	11.07918	15	21.88509
15.5	0.439798	15.5	0.907011	15.5	2.464649	15.5	5.497571	15.5	11.31185	15.5	22.73468
16	0.439756	16	0.907849	16	2.4737	16	5.548851	16	11.5375	16	23.60094
16.5	0.439711	16.5	0.908497	16.5	2.481507	16.5	5.596063	16.5	11.75626	16.5	24.48567
17	0.439669	17	0.909004	17	2.488317	17	5.63958	17	11.96856	17	25.39082
17.5	0.439631	17.5	0.909393	17.5	2.49422	17.5	5.679595	17.5	12.17466	17.5	26.31875
18	0.439603	18	0.90971	18	2.49934	18	5.716403	18	12.37485	18	27.27148
18.5	0.43958	18.5	0.909969	18.5	2.5038	18.5	5.751356	18.5	12.56944	18.5	28.25124
19	0.43956	19	0.910175	19	2.507726	19	5.781668	19	12.75883	19	29.26085
19.5	0.439542	19.5	0.910337	19.5	2.511147	19.5	5.810558	19.5	12.94323	19.5	30.30271

However, the traditional least squares method does not allow researchers to achieve the required target in the case of the mechanical problem studied. Namely, it may happen that only one sudden jump of the shell deformation may yield the shell collapse even when the least squares sum of deviations is small. Furthermore, an introduction of constraints applied to the approximating functions may violate results of the regression analysis. For these reasons another approach is applied. A generalization of the method for data approximation following Chebyshev's investigations [36] is proposed regarding a unique and best approximation of a function through an algebraic polynomial of fixed order, which enables also a detection of additional properties hidden in a dynamic series. Let us note that Vygodchikova [38] investigated problem (4.1) and its potential generalization for approximations of a population number.

The following constraints on the approximating function are applied to problem (4.1):

$$\rho(A)=\max_{k=0,\dots,N}\left|y_k-p_n(A,t_k)\right|\to\min_{A\in D=\{A\in R^{n+1}:p_n(A,t_0)=y_0\}}. \tag{4.3}$$

Remark 1. The constraint introduced in point $t=t_0$ is satisfied within our investigation.

Remark 2. If the approximating polynomial (solution to problem (4.1)) satisfies the constraint $p_n(A,t_0)=y_0$, then this polynomial is a solution to problem (4.3).

Let us analyze applicability of problem (4.3) in order to get quantitative estimations. At the beginning fundamental properties of a solution to problem (4.3) are studied assuming that $N\geq n+1$. An arbitrary set $\sigma=\{t_{j_0}<t_{j_1}<\dots<t_{j_{n+1}}\}\subset T$ with fixed point $t_{j_0}=t_0$, where Ω stands for the set of all bases, is further called a semi-basis.

Since only the semi-bases are used while considering problems (4.3), further in the text the word "semi" is omitted for simplicity. Besides of problem (4.3), the following supplemented issues are considered:

$$\rho_i(A,\sigma)=\max_{k=0,\dots,n+1}\left|y_{j_k}-p_n(A,t_{j_k})\right|\to\min_{A\in D},\quad i\in 0,\dots,1. \tag{4.4}$$

A novel algorithm is derived to find solutions to our problem which differs fundamentally from the existing methods. Our investigations on the application of linear solutions to mini–max problems within the studied class of problems show numerous advantages of our proposed algorithm in comparison to the traditional approaches.

The maximum absolute error of approximation is denoted by $\rho^*=\min_{A\in D=\{A\in R^{n+1}:p_n(A,t_0)=y_0\}}\rho(A)$ and the maximum relative error of approximation by $\Theta^*=\rho^*/\max_{k=0,\dots,N}y_k$. Taking $n=1$, one gets $p_1(A,t)=p_1((a_0,a_1),t)=a_0+a_1t$. In this case, a semi-basis is the set $\sigma=\{t_{j_0}<t_{j_1}<t_{j_2}\}\subset T$ with fixed point $t_{j_0}=t_0$. Hence, problem

(4.3) is equivalent to the following one:

$$\rho(A)=\max_{k=0,\dots,N}\left|y_k-a_0-a_1t_k\right|\to\min_{A\in\{A\in R^2:a_0+a_1t_0=y_0\}} \tag{4.5}$$

Let us consider three new estimating indexing parameters which are applied to quantify the shell deformation development in time versus the load action (owing to the data resulting from the investigation carried out and given in Table 1): ρ^*, Θ^*, a_1. It is observed that the coefficient of polynomial slope of the best approximation a_1 stands for the estimation of data inclination from the stationary function $y_k=y_0$, $k=0,\dots,N$. Then, following the results obtained in Ref. [36], the following theorem can be formulated.

Theorem.. *Solution to problem (4.5) is unique. Vector $A=(a_0,a_1)\in R^2$ is a solution to the stated problem if and only if the following relations hold for semi-basis σ and quantity $h(\sigma)$:*

$$a_0+a_1t_{j_0}=y_0, \tag{4.6}$$

$$y_{j_1}-a_0-a_1t_{j_1}=-h(\sigma), \tag{4.7}$$

$$y_{j_2}-a_0-a_1t_{j_2}=h(\sigma), \tag{4.8}$$

where: $\rho(A)=\left|h(\sigma)\right|$.

Remark. When A and $h(\sigma)$ satisfy the theorem conditions, one has $\rho^*=\left|h(\sigma)\right|$.

Remark. For $t_0=0$, $y_0=0$ one gets $a_0=0$.

The solution to algebraic Eqs. (4.6)–(4.8) is as follows:

$$a_1=\frac{y_{j_1}+y_{j_2}-2y_0}{t_{j_1}+t_{j_2}-2t_{j_0}}, \tag{4.9}$$

$$a_0=y_0-a_1t_{j_0}=\frac{y_o(t_{j_1}+t_{j_2})-t_{j_0}(y_{j_1}+y_{j_2})}{t_{j_1}+t_{j_2}-2t_{j_0}}, \tag{4.10}$$

$$h(\sigma)=y_{j_2}-a_0-a_1t_{j_2}. \tag{4.11}$$

The above theorem is supported with the following example. Let $T=\{0<1<4\}$, $y_0=0$, $y_1=4$, $y_2=8$, then the solution to problem (4.6)–(4.8) be $a_0=0$, $a_1=1.6$, $h=1.6$. The algorithm of solution to the problem requires a multiple solution of Eqs. (4.9)–(4.11) using the choice of target-oriented bases (see [38] for more details).

Further on a concept of the Hausdorff distance is applied to get estimating characteristics which measure a distance between the approximating functions. First, the Hausdorff distance is computed. Consider sets A and B from R^2. They are composed of elements $(t,p(t))$, where $p(t)=a_0+a_1t$ is the approximating polynomial. Let $X(A,B)=\max\left\{\sup_{a\in A}\inf_{b\in B}\rho(a,b);\sup_{b\in B}\inf_{a\in A}\rho(a,b)\right\}$ be the Hausdorff distance between sets A and B, and let $\tilde\rho(w,v)=\max\{|w_1-v_1|,|w_2-v_2|\}$ be the distance between points $w=(w_1,w_2)$ and $v=(v_1,v_2)$ in R^2 in the sense of Minkowski's metrics. Parts of the graphs of linear polynomials $p_1(t)$, $\tilde p_1(t)$, located between points t_0 and t_N as sets A and B can also be taken. Subscript "1" is omitted further in the study.

Table 2
Computation of slopes of experimental functions and associated errors.

Load	a_1 (tan of the approximating function slope)	Maximum error	%
0	0	0	0.00
0.025	0.032546235	0.195109588	44.39
0.05	0.062024607	0.299142497	32.86
0.075	0.162547472	0.65852838	26.22
0.1	0.351824913	1.050027343	18.07
0.125	0.717227702	1.042710768	8.06
0.15	1.431082975	2.396594933	7.91

The required steps of estimation of the Hausdorff distance between points of linear functions are taken. Consider interval $[t_0,t_N]$ and two linear functions $p(t)=a_0+a_1t$, $\tilde p(t)=c+dt$ (assume that $|a_1|\ge|d|$). The Euclidean distance between parts of these functions located between points t_0 and t_N is defined by the following formula:

$$e(Grp,Gr\tilde p)=\max\{\left|(a_0-c+t_0(a_1-d))\cos(\arctan|a_1|)\right|,\ \left|(a_0-c+t_N(a_1-d))\cos(\arctan|a_1|)\right|\}, \tag{4.12}$$

whereas the Hausdorff distance is given by the following equation:

$$X(Grp,Gr\tilde p)=e(p,\tilde p)\max\{\cos(\arctan|a_1|),\ \sin(\arctan|a_1|)\}. \tag{4.13}$$

Both quantities (4.12)–(4.13) presented so far will be applied while estimating a distance between graphical pictures of the deformation development for various loads applied. In order to obtain the required target the real data are substituted by the computational counterpart data using model (4.5).

5. Computational experiment

The values of displacements on each chosen load level with variation in time t are approximated by a linear function dependent on t in the constraint introduced at zero, and formulas (4.9)–(4.11) are used. As a result, a coefficient of the slope of the approximating linear function is found and a maximum error of approximation regarding both absolute and relative measurements is derived (Table 2).

To get a physical explanation of the deformation developed in time for different load levels, the values of approximating polynomials $p(t)=a_1t$ on each load level are computed. The values obtained experimentally (Table 1) are substituted by smoothened values obtained via approximating functions. Collecting results of the deformation developed for load levels 0.025, 0.05, 0.075, 0.1, 0.125, 0.15, the approximating function for each level, shown in Fig. 10, is obtained.

Remark. The loads used for visualization and function slopes are given in Table 3.

Below, computation of a critical load is illustrated and discussed. An increase of the load (higher than 0.05) is accompanied by a sudden change in deformation velocity a_1, whereas the error of approximation in percentage is decreased. This is because the deflection increase regarding its maximum value is decreased due to a sudden increase of the deformation velocity of the shell deflection. The increase of the load from 0.1 to 0.125 causes an increase of the deformation velocity in more than 100% (the deformation process is out of control, since the increase of deflection magnitude with respect to its maximum value became negligible comparing with the increase of the sudden deformation

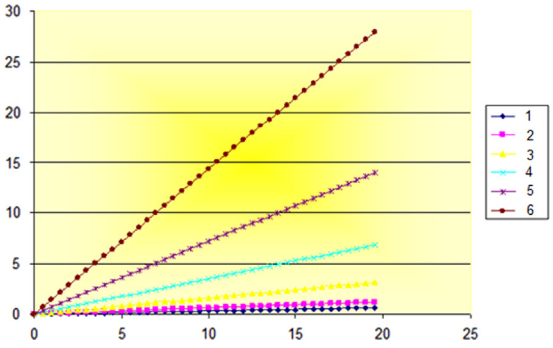

Fig. 10. Graphs of the approximating functions for different loads (numbers denote applied series).

velocity). The loading described so far is referred to as a critical one (stabilization of the error in percentage with an increase of a_1 is observed) – see Table 4.

The estimated critical load achieves the value of 0.125, which is in full agreement with the results obtained by the method of relaxation (Fig. 3).

The increase in development of shell deformation velocity versus load increase is evident (see Table 4). In order to illustrate quantification of this process for various loading ways, a distance between the approximation functions for different loading series computed using formulas (4.12) and (4.13) were monitored and estimated. This leads to a conclusion that a sudden buckling takes places for the load 0.125 (see Table 5).

6. Concluding remarks

In this work critical load values were estimated while analyzing the stability of spherical circle axially symmetric shells using the relaxation method. In order to solve static problems of the theory of plates and shells usually numerous approximating methods are applied aiming at a reduction of ODEs to NAEs which are then linearized. On the other hand, the relaxation method is used to reduce the investigated PDEs to a Cauchy problem of ODEs. As a result of the mentioned analysis one may get various graphical stress–strain representations of the mechanical objects studied. Though they are very helpful in particular at the first step of the study, they are not sufficient to fully understand and characterize the analyzed processes, to compare dynamic processes exhibited by different shells, and to monitor health of the analyzed processes in different periods of their life. This was a motivation to propose qualitatively novel estimating characteristics, following and modifying the classical Chebyshev's approach.

The proposed approach has the following advantages:

(i) *High target information*: even minimum values of a target function transform the important information regarding the maximum absolute error of initial data approximation (in our case it is a linear function). The mentioned high target information property is preserved even at the lack of tendency to stability of the studied process.

Table 3
Series number, loading values and coefficient a_1.

Series	Load	a_1	Angle (deg.)
1	0.025	0.032546235	1.864103919
2	0.05	0.062024607	3.549201552
3	0.075	0.162547472	9.232536168
4	0.1	0.351824913	19.38314222
5	0.125	0.717227702	35.64913893
6	0.15	1.431082975	55.05524717

Table 4
Computation of the critical load level, where Θ*% is the maximum error of linear approximation (%).

Series	Load	a_1		Θ* [%]	
	0	0		0	
1	0.025	0.03255		44.39	
2	0.05	0.06202		32.86	
3	0.075	0.16255		26.22	
4	0.1	0.35182		18.07	
5	0.125	0.71723	increase	8.06	stabilization
6	0.15	1.43108		7.91	

Table 5
Critical load estimation (second way).

Load approximation		Euclidean distance	Hausdorff distance	Relative increase (%)
0.025	0.05	0.573725733	0.572625331	0.19
0.05	0.075	1.934802137	1.909737386	1.31
0.075	0.1	3.481710603	3.284368454	6.01
0.1	0.125	5.790071619	4.705019218	23.06
0.125	0.15	7.973287237	6.535741274	22.00

(ii) *Possibility of high data compression*: in the case of a stable dynamic process a large choice of data is substituted by only two coefficients of the polynomial of best approximation. Though the latter approach is similar to the standard least squares procedure, a large volume of the gathered data can be truncated to only two values corresponding to the extremum of the studied problem with a constraint.

(iii) Dependence of the solution on the values of measuring parameter applied in a few considered points only (without taking into account other remaining data) does not violate predicting property of the parameter, and the error of approximations remains unaffected. This property may be applied to smooth the data.

(iv) Results can be easily validated, and the method is mathematically approved and clearly interpreted.

Finally, the following estimating characteristics of the graphical pictures are obtained: (i) velocity of a linear deformation developed in time with regard to the initial loading action; (ii) maximum absolute and relative errors of data approximation regarding the development of deformation using linear functions; (iii) distance between data series regarding deformation for different loads obtained via approximation of the mentioned series by linear functions.

Basing on the analysis of the mentioned indices, the level of critical load for experimentally obtained data has been defined. The results validate also algorithms and theoretical background of the applied relaxation method.

Acknowledgment

The work has been financially supported by the RFF grant (Project no. 13-01-00175) and by the National Science Centre of Poland under the grant MAESTRO 2 No. 2012/04/A/ST8/00738 for the years 2013–2016.

References

[1] Smitses GJ. Instability of dynamically loaded structures. Appl Mech Rev 1987;40(10):1403–8.
[2] Timoshenko SP, Gere JM. Theory of Elastic Stability. New York: McGraw-Hill; 1961.
[3] Volmir SA. Stability of Deformable Systems. Moscow: Science; 1967 in Russian.
[4] Volmir SA. Nonlinear Dynamics of Plates and Shells. Moscow: Science; 1972 in Russian.
[5] Kubiak T. Static and Dynamic Buckling of Thin-Walled Plate Structures. Berlin: Springer; 2013.
[6] Davids AJ, Hancock GJ. Compression tests of long welded I-section columns. J Struct Eng 1986;112(10):2281–97.
[7] Graves-Smith TR. The postbuckled behavior of a thin-walled box beam in pure bending. Int J Mech Sci 1972;14:711–22.
[8] Grimaldi A, Pignataro M. Post-buckling behavior of thin-walled open cross-section compression members. J Struct Mech 1979;7(2):143–59.
[9] Koiter WT. Elastic stability and post-buckling behavior. Proceedings of the Symposium on Non-Linear Problems. Wisconsin: University of Wisconsin Press; 1963. p. 257–75.
[10] Byskov E, Hutchinson JW. Mode interaction in axially stiffened cylindrical shells. AIAA J 1977;15(7):941–8.

[11] Byskov E. Elastic buckling problem with infinitely many local modes. Mech Struct Mach 1988;15(4):413–35.
[12] Pignataro M, Luongo A. Asymmetric interactive buckling of thin-walled columns with initial imperfection. Thin-Walled Struct 1987;3:365–85.
[13] Chang F. Sci Sin 1958;VII:716.
[14] Reissner E, Stavsky Y. Bending and stretching of certain types of heterogeneous allotropic elastic plates. Trans ASME J Appl Mech 1961;9:402–8.
[15] Ambartsumyan SA. Theory of anisotropic plates. Technomic, Stamford, Conn; 1970.
[16] Ashton JE, Whitney JM. Theory of laminated plates. Technomic, Stamford, Conn; 1970.
[17] J.M. Mandell, An experimental study of the postbuckling of anisotropic plates [MSc thesis], 1968, Case Western Reserve University, Cleveland, Ohio.
[18] Chailleux A, Hans Y, Verchery G. Experimental study of the buckling of laminated composite columns and plates. Int J Mech Sci 1975;17:489–98.
[19] Chandra R, Raju B. Postbuckling analysis for rectangular orthotropic plates. Int J Mech Sci 1973;16:81–97.
[20] Budiansky B and Roth RS, Axisymmetric dynamic buckling of clamped shallow spherical shells, Collected Papers on Instability of Shell Structures, 1962, NASA TN D -1510, Washington, DC, 597-606.
[21] Hutchinson JW, Budiansky B. Dynamic buckling estimates. AIAA J 1966;4-3:525–30.
[22] Budiansky B., Roth R.S., Axisymmetric dynamic buckling of clamped shallow spherical shells, Collected Papers on Instability of Shell Structures, 1962, NASA TN D -1510, Washington, DC, 597-606.
[23] Ari-Gur J, Simonetta SR. Dynamic pulse buckling of rectangular composite plates. Compos B 1997;28B:301–8.
[24] Petry D, Fahlbusch G. Dynamic buckling of thin isotropic plates subjected to in-plane impact. Thin-Walled Struct 2000;38:267–83.
[25] Kulikov GM. Numerical investigation of the material strength of composite rotational shells with complex forms. Izv. USSR Acad. Sci MTT 1981;4:192 in Russian.
[26] Valishvili NV. Numerical Methods of Rotational Shells Computation. Moscow: Mashinostroyeniye; 1976 in Russian.
[27] Feodos'ev VI. On a method of solution of stability of deformed bodies. PMM 1963;27(2):265–75.
[28] Awrejcewicz J, Krysko VA, Nazar'iantz V. Chaotic vibrations of flexible infinite length cylindrical panels using the Kirchhoff–Love model. Commun Nonlinear Sci Numer Simul 2007;12(4):519–42.
[29] Awrejcewicz J, Krysko VA, Saveleva NE. Routes to chaos exhibited by closed flexible cylindrical shells. J Comput Nonlinear Dyn 2007;2(1):1–9.
[30] Krysko VA, Awrejcewicz J, Saveleva NE. Stability, bifurcation and chaos of closed flexible cylindrical shells. Int J Mech Sci 2008;50(2):247–74.
[31] V.V. Novozhilov, Theory of thin shells, 1959, P. Noordhoff, Groningen.
[32] Reissner E. Stresses and small displacements of shallow spherical shells. J Math A Phys 1946;25:80–5.
[33] Vlasov VZ. General Theory for shells and its application in engineering. Moscow: Gostekhizdat Publ; 1949.
[34] Awrejcewicz J, Krysko VA. Nonclassical thermoelastic problems in nonlinear dynamics of shells. Berlin Heidelberg: Springer-Verlag; 2003.
[35] Krysko VA, Awrejcewicz J, Komarov SA. Nonlinear deformations of spherical panels, subjected to transversal load action. Computer Methods Appl Mech Eng 2005;194:3108–26.
[36] Demianov VF, Malozemov VN. Introduction into minimax. Moscow: Nauka; 1972 in Russian.
[37] Krysko VA, Awrejcewicz J, Kutepov IE, Vygodchikoval IYu, Krysko AV. Quantifying chaos of curvilinear beam via exponents. Commun Nonlinear Sci Numer Simul 2015;27(1-3):81–92.
[38] I.Yu. Vygodchikova, On the method of approximation of economical data using the Chebyshew approach and its generalization, Izvestia of the Saratov National University, 12, 2012, 77-80.